Polymer Chemistry

ROYAL SOCIETY OF CHEMISTRY

PAPER

View Article Online
View Journal | View Issue

Cite this: *Polym. Chem.*, 2023, **14**, 763

A tridentate phenoxy-phosphine (POP) divalent chromium complex and its reactivities in olefin polymerization†

Li Ji,[a] Ping Song,[a] Youyun Zhou,*[a] Xiu-Li Sun,[b] Yanshan Gao*[b] and Yong Tang*[a,b]

We reported the synthesis and characterization of a Cr(II) complex based on a tridentate phenoxy-phosphine ligand and comprehensively studied its reactivities in ethylene and norbornene homopolymerization and ethylene copolymerization with norbornene or 1-octene. Upon methylaluminoxane (MAO) activation, the precatalyst catalyzes ethylene polymerization with activities up to 331.7 kg (mol cat h)$^{-1}$. The polyethylene (PE) M_w and dispersity ($Đ$) can be flexibly tuned, ranging from predominantly high molecular weight (HMW, 42.3 kg mol^{-1}, 97.5 wt%) to mostly low molecular weight (LMW, 1.8 kg mol^{-1}, 94.8%), and from bimodal to nearly monomodal *via* changing MAO loadings and reaction temperatures. End group analysis by NMR shows β-H elimination as the major chain termination pathway *vs.* chain transfer to $AlMe_3$ as a minor pathway, forming vinyl-terminated PE and saturated PE, respectively; in the cases where vinyl-terminated LMW PE is formed, vinylidene and 1,2-substituted internal olefinic end groups can be observed at the expense of chain end vinyl and methyl groups. In norbornene homopolymerization, the catalytically active site is incapable of undergoing β-H elimination and shows single-site catalytic behavior with chain transfer to $AlMe_3$ as the sole chain transfer/termination pathway, which is confirmed by polymer NMR and MAO loading experiments. Interestingly, the catalyst system also exhibits single-site catalytic behavior in all the ethylene copolymerization experiments with NBE and 1-octene monomers as shown by copolymer GPC and NMR (^{1}H, ^{13}C, DEPT, HMBC) studies, and exhibits unique monomer effects on catalytic behavior in terms of comonomer enchainment selectivity, M_w, and chain transfer/termination processes. The active species under different conditions were studied by UV-vis-NIR.

Received 30th November 2022,
Accepted 7th January 2023

DOI: 10.1039/d2py01509a

rsc.li/polymers

Introduction

The discovery of the Phillips chromium catalyst (CrO_3/SiO_2) by Hogan and Banks (Phillips Petroleum) in the 1950s is a milestone in the polyolefin industry, and this heterogeneous catalyst system still accounts for 40–50% of the global production of high-density polyethylene (HDPE).[1–4] Developing new homogeneous Cr catalyst systems for olefin polymerization with greater efficiency and selectivity in terms of M_w, dispersity ($Đ$), branch density, *etc.* has been an attractive goal for both academic and industrial research in the past decades.[5–7] However, these efforts are far less successful than group IV Ti/Zr/Hf homogeneous catalysis following Ziegler–Natta discoveries in the 1950s.[8–14]

Cyclopentadienyl (Cp)-based Cr complexes represent an important kind of well-defined homogeneous catalyst, many of which show high reactivity and produce high molecular weight PEs in olefin polymerization.[15–20] Besides, non-Cp ligands have attracted special attention because of the large variety of ligand structural motifs and flexible tunability of the catalysts' steric and electronic properties.[7,21] Bidentate and tridentate ligands with hard donors (N and O) have been developed, such as bis(imino)pyridine,[22–24] nacnac,[25] and phenoxy-imino-amine[21,26] catalysts, and these ligands allow modulation of the polymers M_w from the ethylene oligomer (PE wax) to HDPE, with moderate to high activities. Introducing soft donors [S and P] into ligand design realized not only highly selective ethylene oligomerization[27–31] but also ethylene polymerization affording PEs with various molecular weights.[32–34]

These representative catalyst systems suggest that designing new ligand/Cr catalysts particularly based on mixed hard and

[a]*Shenzhen Grubbs Institute and Department of Chemistry, and Guangdong Provincial Key Laboratory of Catalysis, Southern University of Science and Technology, Guangdong, China. E-mail: zhouyy@sustech.edu.cn*
[b]*State key Laboratory of Organometallic Chemistry, Shanghai institute of Organic Chemistry, Chinese Academy of Sciences, Shanghai, China. E-mail: tangy@sioc.ac.cn, gaoyanshan@sioc.ac.cn*

†Electronic supplementary information (ESI) available: Experimental details of catalyst synthesis/characterization, crystallographic details (CIF), polymerization experiments, and polymer characterization by NMR and GPC. CCDC 2205183. For ESI and crystallographic data in CIF or other electronic format see DOI: https://doi.org/10.1039/d2py01509a

soft multidentate donors is still a powerful strategy for developing high-performance Cr catalysts. Meanwhile, compared with Cr(III) catalyst, Cr(II) catalyst received much less attention. Gambarotta investigated a series of concerted and single-component Cr(II) catalysts,[35–37] and most of them exhibit high selectivity for ethylene trimerization. A limited number of Cr(II) catalysts were reported to show catalytic activity for reactions such as 1,3-diene polymerization[38] and selective ethene oligomerization,[39–41] and in some cases, the Cr(II) complexes are inactive *vs.* their highly active Cr(III) analogs under the same conditions.[23,42] We embarked on a project to design divalent Cr catalysts, explore their catalytic reactivities in various olefin polymerization reactions and synthesize polyolefins with diversified and well-controlled microstructures. Here we report a Cr(II) catalyst with a tridentate phenoxy-phosphine (POP) ligand. We comprehensively studied its catalytic behavior in terms of M_w, $Đ$, comonomer enchainment selectivity, and chain termination/transfer processes in ethylene, octene and norbornene polymerization, and successfully synthesized a series of polyolefins with well-controlled and diversified microstructures and compositions.

Results and discussion

Synthesis of Cr complex cat.1

The POP-tridentate ligand **L1** was prepared following the procedure reported in the literature.[43] We then tried the synthesis of the bimetallic Cr complex. The ligand **L1** was deprotonated with 1.2 equiv. of KH and then reacted with 2.0 equiv. of $CrCl_2$ to afford the green Cr(II) complex **cat.1** (Scheme 1). Single crystals suitable for X-ray diffraction studies were grown by slow diffusion of *n*-hexane into a solution of **cat.1** in THF in the freezer of a glovebox. Note that this complex underwent a quick color change from green to black once exposed to air and was handled under oxygen- and moisture-free conditions.

The solid-state structure of **cat.1** shows a distorted square pyramidal geometry[44,45] around the Cr metal center with the basal plane defined by the P and O atoms from the POP ligand and two Cl atoms (Fig. 1). It is C_2-symmetric and prime marks are used for labeling the atoms in Fig. 1 for the convenience of discussion. The POP ligand is bidentate to both Cr atoms, which share the same bridging O atom with a bond distance of 2.0205(10) Å for Cr1–O1. There is also a bridging Cl atom with a bond distance of 2.4203(5) Å for Cr1–Cl2 *vs.* 2.3074(5) Å for the Cr1–Cl1 bond with the non-bridging Cl atom, both comparable to the corresponding bond distances reported in

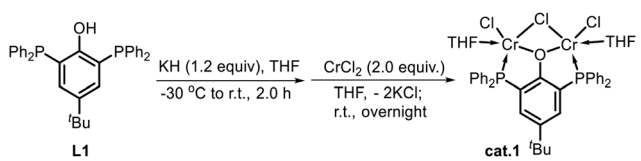

Scheme 1 Synthesis of **cat.1**.

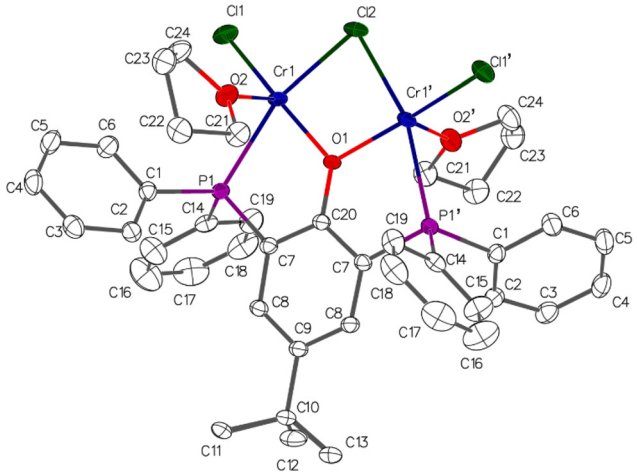

Fig. 1 Solid state structure of **cat.1**. Hydrogen atoms are omitted for clarity.

the literature.[22,26,32,33,46–48] The Cr1···Cr1′ distance is 3.271 Å, which is among those of previously reported bimetallic Cr complexes [2.27–3.49 Å].[49–52] The two chelating rings (Cr1–O1–C20 and Cr1′–O1–C20) are in the same plane (dihedral angle = 0°). The other two chelating rings (P1–Cr1–O1 and P1′–Cr1′–O1) are almost coplanar with a dihedral angle of 4.198°, and the benzene rings connected with P atoms are pointed away from the metal center, both contributing to a relatively open coordination environment for the two Cr centers.

Next, we carried out olefin polymerization to study the catalytic behavior of **cat.1** in polymerizing various monomers such as ethylene, 1-octene, norbornene, or their combinations. The precatalyst is barely soluble in toluene even after mixing with excess aluminoxane (MAO, MMAO, and $AlEt_2Cl$) or trialkylaluminum ($AlMe_3$ and Al^iBu_3) in toluene. Thus, 10 mL of PhCl was used to dissolve the precatalyst for activation, and toluene was used as the major solvent in all the polymerization experiments.

Ethylene polymerization

The effects of cocatalysts and their loading on ethylene polymerization were first explored. After optimization, we studied the effects of temperature on ethylene polymerization. This catalyst system exhibits well-controlled PE product dispersity from bimodal to monomodal, indicating single or dual-site catalytic behavior.

Type of cocatalyst. The cocatalyst plays a key role in the alkylation of the precatalyst and the subsequent alkyl abstraction to form the cationic Cr–R species.[26,32,33,53] Therefore, various Al reagents such as MAO, MMAO, $AlEt_2Cl$, $AlMe_3$, and Al^iBu_3 were first evaluated (Table 1). A productive run was obtained only when MAO was used. With 2000 equiv. of MAO per Cr at 50 °C, **cat.1** efficiently polymerizes ethylene with an activity of 309.0 kg (mol cat h)$^{-1}$ (entry 5, Table 1). The product PE shows a bimodal molecular weight distribution. Deconvolution of the GPC trace of this bimodal PE was carried out to quantify the

Table 1 **Cat.1** catalyzed ethylene homopolymerization[a]

Entry	Cocat.	Cocat. equiv./Cr	C_2H_4/atm	T/°C	Yield/g	Act.[b]	M_w (HMW)[c]	$Đ$ (HMW)[c]	M_w (LMW)[c]	$Đ$ (LMW)[c]	wt % (LMW)[c]
1	$AlEt_3$	2000	10	50	Trace	—	—	—	—	—	—
2	Al^iBu_3	2000	10	50	Trace	—	—	—	—	—	—
3	$AlEt_2Cl$	2000	10	50	Trace	—	—	—	—	—	—
4	MMAO	2000	10	50	Trace	—	—	—	—	—	—
5	MAO	2000	10	50	0.772	309.0	44.7	2.7	1.7	1.2	43.5
6	MAO	500	10	50	0.114	45.7	24.6	1.6	1.8	1.2	94.8
7	MAO	1000	10	50	0.230	92.0	19.4	1.6	1.6	1.2	78.2
8	MAO	3000	10	50	0.792	316.9	33.9	3.4	1.3	1.1	9.2
9	MAO	2000	10	0	0.307	122.8	41.5	2.9	1.7	1.1	3.3
10	MAO	2000	10	30	0.829	331.7	42.3	3.1	0.4	1.0	2.5
11	MAO	2000	10	80	0.641	256.4	39.1	2.2	1.9	1.2	74.3
12	MAO	2000	10	100	0.477	190.8	32.3	2.1	1.5	1.3	92.5
13	MAO	2000	10	120	Trace	—	—	—	—	—	—
14	MAO	2000	1	50	Trace	—	—	—	—	—	—
15	MAO	2000	5	50	Trace	—	—	—	—	—	—

[a] Conditions: **cat.1**, 5.0 μmol; PhCl, 10 mL; toluene as the solvent, total volume 50 mL; ethylene, 10 atm; reaction time, 0.5 h. All reactions were performed at least in duplicate. [b] kg (mol cat h)$^{-1}$. [c] Determined by GPC *vs.* polystyrene standards, kg mol^{-1}. HMW = high M_w fraction; LMW = low M_w fraction. Weight percentage of LMW (wt%) was calculated based on the deconvolution of polymer GPC traces. The narrow $Đ$ likely reflects the inaccuracy related to the GPC's low M_w detection limit.

weight percentages of low molecular weight (LMW) and high molecular weight (HMW) fractions, which are fitted with two Schulz–Flory peaks independently for M_w and polymer dispersity.[54] Meanwhile, processing the GPC trace separately allows quantification of the M_w of each fraction. The above sample contains 56.5 wt% HMW fraction (M_w = 44.7 kg mol^{-1}, $Đ$ = 2.7) and 43.5 wt% LMW fraction (M_w = 1.7 kg mol^{-1}, $Đ$ = 1.2). The catalyst's bimodal behavior likely suggests that two active sites exist in the catalyst system. Note that ethylene polymerization at reduced pressure (5 atm and 1 atm) leads to inactivity due to the unstable nature of the *in situ* generated active species and the stabilizing effects of the olefin monomer.[22,55] Next, we investigated the effects of MAO loading and reaction temperature on catalysis to better understand the precatalyst **cat.1**'s catalytic behavior.

MAO loading. The amount of MAO per catalyst shows remarkable effects on both catalytic activity and the weight percentages of LMW and HMW fractions. Increasing the MAO/Cr loading from 500 to 3000 equiv. led to enhanced activity (by 6.9×), which can reach up to 316.9 kg (mol cat h)$^{-1}$ when 3000 equiv. of MAO/Cr were used at 50 °C (entry 8, Table 1). Interestingly, the ratio of the LMW fraction decreases with increasing MAO loading, from a predominant LMW fraction (94.8 wt%) to a predominant HMW fraction (90.8 wt%) when 500 and 3000 equiv. of MAO/Cr were used, respectively (Fig. 2a). The switched molecular weight capability and dispersity likely reflect the varied catalytically active sites generated in the presence of varied MAO loadings.[32] ^{1}H and ^{13}C NMR spectra of the bimodal PE from entry 5 Table 1 show exclusive vinyl end group unsaturation and a linear microstructure (Fig. S3 and S4†) and exclude the possibility of re-enchainment of the *in situ* formed vinyl-terminated macromonomer, which was proposed as a viable pathway toward bimodal polymers.[56,57]

Temperature. The reaction temperature influences catalyst performance in terms of activity, and product polymer's molecular weight and dispersity. When the oil bath temperature was increased from 0 to 30 °C, the activity increased from 122.8 to 331.7 kg (mol cat h)$^{-1}$ (entries 9 and 10, Table 1), and further increasing the temperature to 100 °C led to a gradually decreased activity, indicating catalyst deactivation at higher temperatures. Interestingly, reaction temperature shows remarkable effects on polymer dispersity and ratios of the LMW and HMW fractions in the bimodal polymer. The bimodal PE changed from the predominant HMW fraction (96.7 wt%, entry 9, Table 1) to the predominant LMW fraction

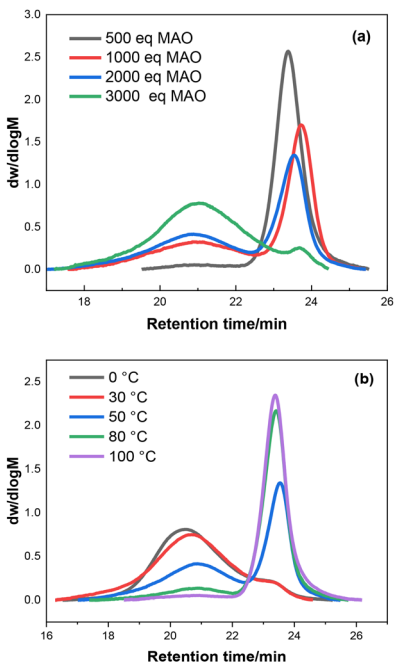

Fig. 2 Effects of MAO loading (a) and polymerization temperature (b) on PE molecular weight (M_w) and dispersity ($Đ$).

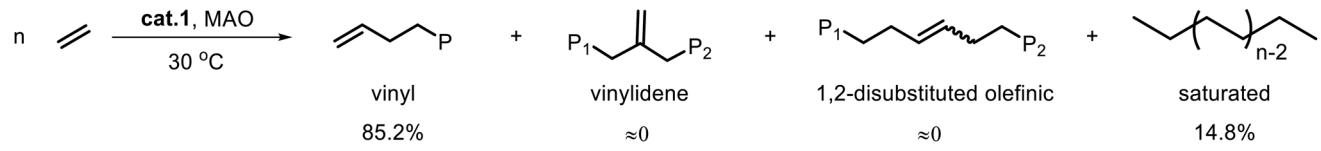

Scheme 2 PE products with various chain end olefinic and methyl groups in **cat.1**/MAO catalyzed ethylene polymerization (2.5 wt% LMW and 97.5 wt% HMW; entry 10, Table 1). P, P1 and P2 indicate the polymer chain.

(92.5 wt%, entry 12) when the temperature was increased from 0 to 100 °C (Fig. 2b). The switch of the near single-site catalytic behavior and the resulting PE product M_w was successfully realized with **cat.1** through the effects of reaction temperature. The polymer molecular weight is proportional to the rate ratios of chain propagation/chain termination processes.[58] Chain termination occurs *via* two possible pathways, *i.e.* β-H elimination and chain transfer to $AlMe_3$ (from MAO). In cases where both pathways exist, end group analysis *via* ^{1}H NMR can quantify their ratios.[59,60] In this work, we compared the ethylene polymerization with **cat.1**/MAO (2000 equiv.per Cr) at 30 °C and 100 °C, which afforded PE products with predominant HMW and predominant LMW fractions, respectively. PE products with various chain end olefinic and methyl groups determined from ^{1}H NMR characterization (Fig. S5 and S6†) are shown in Scheme 2. The PE product obtained in the 30 °C reaction (entry 10, Table 1) is predominantly high molecular weight (97.5 wt% HMW fraction), and end group analysis shows 85.2% vinyl-terminated PE *vs.* 14.8% saturated (methyl-terminated) PE, corresponding to the ratio of β-H elimination *vs.* chain transfer to $AlMe_3$. The PE product obtained in the 100 °C reaction (entry 12, Table 1) is predominantly low molecular weight (92.5 wt% LMW fraction), and end group analysis shows the major olefinic end group and minor methyl end groups. The different chain end group features as well as the M_w and $Đ$ trends are likely due to the combined effects of different *in situ* formed active species and reaction temperatures. Interestingly, certain amounts of vinylidene and 1,2-disubstituted olefinic end groups were also observed in the PE sample obtained in the 100 °C polymerization, which is likely due to the β-H elimination after enchaining the *in situ* formed low M_w vinyl-terminated ethylene oligomers (Fig. S6†). Note that the above analysis is based on the bimodal PE products from the 30 °C polymerization, which reasonably reflects two active sites' average catalytic behavior and chain termination/transfer preference disregarding each site's independent contribution. We have shown the variable factors that allow efficient modulation of the resulting PE's modality, from monomodal to bimodal. It is worth mentioning that bimodal PEs usually have the advantage of easier processing and altering tensile strength *vs.* monomodal HDPE type polymers.[61–64]

NBE homopolymerization and copolymerization with ethylene

To further probe the reactivity of **cat.1** in terms of polymer dispersity and chain end groups, we investigated norbornene (NBE) homopolymerization and ethylene copolymerization with NBE and 1-octene (Table 2). We chose the NBE monomer as it doesn't undergo β-H elimination during homopolymerization.[65,66] For NBE homopolymerization, there are two types of β-H atoms available for the Cr active site, H_a and H_b. H_a is a bridgehead proton making β-H elimination impossible; H_b is *anti* to the Cr active site and the resulting double bond is highly strained, both making β-H elimination impossible. Thus, it allows us to further probe the Cr species' reactivity in terms of product polymer's molecular weight, dispersity, and chain end group (*via* the chain transfer to AlR_3 process[67–70]) in the absence of the β-H elimination process (Scheme 3a).

Norbornene homopolymerization was carried out using **cat.1**/MAO (2000 equiv. per Cr) under 1.0 atm N_2 atmosphere at 30 °C, giving polynorbornene (PNBE) with an activity of 50.4 kg (mol cat h)$^{-1}$. In contrast to ethylene polymerization

Table 2 **Cat.1** catalyzed ethylene, 1-octene and norbornene polymerization[a]

Entry	MAO (equiv. per Cr)	C_2H_4 (atm)	Monomer (mmol)	T/°C	Yield/g	Act.[b]	Incorp. (mol%)[c]	M_w[d]	M_n[d]	$Đ$[d]	Chains/cat
1	2000	—	NBE (40)	30	0.126	50.4	—	2.0	1.6	1.3	16
2	2000	—	NBE (40)	100	0.668	267.2	—	1.5	1.3	1.2	103
3	1000	—	NBE (40)	100	0.523	209.1	—	3.3	2.1	1.6	50
4	500	—	NBE (40)	100	0.358	143.2	—	4.4	2.4	1.9	30
5	250	—	NBE (40)	100	0.133	53.1	—	5.9	3.0	2.0	9
6	100	—	NBE (40)	100	Trace	—	—	—	—	—	—
7	2000	10	NBE (40)	30	2.549	1019.4	66.67	<1	—	—	—
8	2000	10	NBE (40)	100	1.70	680.0	45.77	<1	—	—	—
9	2000	10	1-Octene (60)	30	0.221	88.2	0.83	17.3	4.7	3.7	9
10	2000	10	1-Octene (60)	100	0.150	59.9	0.32	1.9	1.5	1.3	20

[a] Conditions: **cat.1**, 5.0 μmol; MAO, 2000 equiv. per Cr; 10 mL PhCl, toluene as the solvent, total volume 50 mL, 0.5 h. All reactions were performed at least in duplicate. [b] kg (mol cat h)$^{-1}$. [c] Determined by ^{13}C NMR. [d] Determined by GPC *vs.* polystyrene standards, kg mol^{-1}. The narrow $Đ$ likely reflects the inaccuracy related to the GPC's low M_w detection limit.

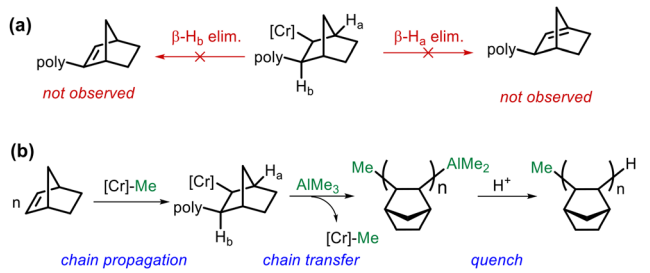

Scheme 3 **Cat.1** catalyzed norbornene homopolymerization. The absence of β-H elimination (a); chain propagation and regeneration of active [Cr] species after chain transfer with $AlMe_3$ (b). [Cr]–Me indicates the active species generated from **cat.1**/MAO.

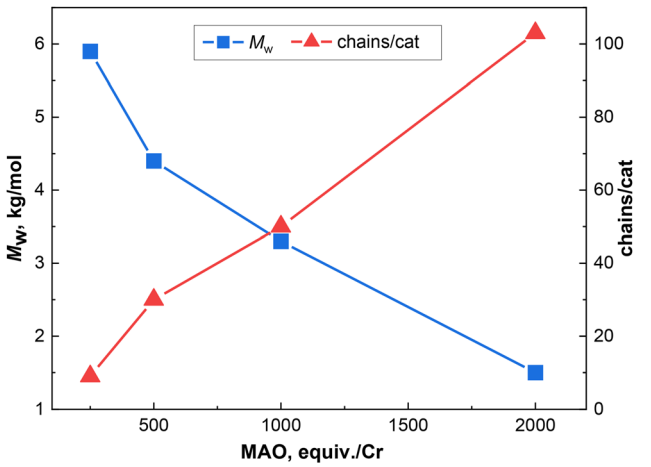

Fig. 3 Effects of MAO loading on **cat.1**/MAO catalyzed NBE homopolymerization.

under identical conditions, which afforded a polymer with bimodal dispersity and a predominant high M_w fraction (97.5 wt% HMW, 42.3 kg mol^{-1}, entry 10, Table 1), the resulting PNBE was a monomodal ($Đ$ = 1.3) NBE oligomer with M_w = 2.0 kg mol^{-1} (entry 1, Table 2). Increasing the reaction temperature to 100 °C led to greatly enhanced activity by ~5× times to 267.2 kg (mol cat h)$^{-1}$ while maintaining monodispersity ($Đ$ = 1.2) and low M_w = 1.5 kg mol^{-1} (entry 2, Table 2), likely owing to the good thermal stability of the catalytically active Cr species and lowered monomer insertion barrier at a higher temperature.

Based on the polymer yield and number-average molecular weight (M_n), about 103 polymer chains per catalyst were generated (entry 2, Table 2), suggesting extensive chain transfer during the NBE polymerization process. Close examination of the polymer ^{1}H NMR showed a lack of chain end olefinic groups, which suggests the lack of β-H elimination as a chain termination pathway and thus chain transfer to $AlMe_3$ (from excess MAO) is likely the chain termination pathway (Scheme 3b). To assess if there is chain transfer to $AlMe_3$, we tried NBE polymerization with varied MAO loadings. When the amount of MAO was gradually reduced from 2000 to 250 equiv. per Cr, a progressive increase of polymer M_w from 1.5 to 5.9 kg mol^{-1} and a decrease in the number of polymer chains per catalyst from 103 to 9 were observed (entries 2–5, Table 2 and Fig. 3). This confirms chain transfer to $AlMe_3$ as the predominant chain transfer pathway in **cat.1** catalyzed NBE homopolymerization. Moreover, ^{1}H, ^{13}C NMR, and DEPT spectra of the PNBE product show peaks that are assigned to the terminal methyl group (Fig. S8–S10†), further supporting the chain transfer to $AlMe_3$ process.[70]

In view of the **cat.1**/MAO catalyst system's distinct monomodal and bimodal catalytic behavior for NBE and ethylene homopolymerization, respectively, we were curious about their copolymerization under identical conditions. NBE copolymerization with ethylene was investigated with **cat.1**/MAO at 30 °C and 100 °C. Remarkably, the activity is as high as 1019.4 kg (mol cat h)$^{-1}$ at 30 °C and 680.0 kg (mol cat h)$^{-1}$ at 100 °C. The NBE incorporation ratios are 66.67 and 45.77 mol%, respectively. GPC measurement shows that their M_w is less than 1 kg mol^{-1}, which exceeds the detection limit. Even though the M_w and M_n data obtained from the GPC traces (Fig. S37 and S38†) are inaccurate, both samples show monomodal and single-site behavior, agreeing with the NBE homopolymerization results.

Polymer ^{1}H NMR suggests the presence of two types of vinyl end groups in the ethylene/NBE copolymer samples, which can be assigned to V_E and V_N.[71] The assignment is further confirmed by combined ^{1}H, ^{13}C, DEPT, and HMBC characterization (Scheme 4 and Fig. S14–S17†).[70] The E-NBE copolymer M_w is lower than that of the NBE homopolymer, likely reflecting β-H elimination as an additional chain termination pathway following ethylene monomer enchainment. While the messy peaks in the copolymer ^{13}C NMR spectra (Fig. S15†) prevent further microstructural analysis, characteristic methyl end groups were observed in the NMR spectra.

Ethylene + 1-octene copolymerization

We also studied **cat.1**'s reactivity toward ethylene/1-octene copolymerization (Table 2). In stark contrast to ethylene homopolymerization, which yields a bimodal polymer with a predominant HMW fraction (M_w = 42.3 kg mol^{-1}, 97.5 wt% HMW, entry 10, Table 1) at 30 °C and a predominant LMW fraction (M_w = 1.5 kg mol^{-1}, 92.5 wt% LMW, entry 12, Table 1) at 100 °C, monomodal copolymers were obtained at both 30 °C and 100 °C with M_w = 17.3 and 1.9 kg mol^{-1}, respectively (entries 9 and 10, Table 2). This suggests single-site catalytic

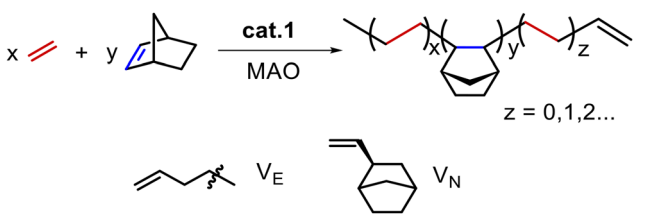

Scheme 4 **Cat.1**/MAO catalyzed ethylene copolymerization with norbornene and the olefinic end groups.

behavior after introducing the 1-octene comonomer. The high concentration of olefin monomers (ethylene and 1-octene) likely promotes the coordination to the Cr metal center and thus stabilizes the metal center during precatalyst alkylation/activation and catalysis processes.[72] The precatalyst's alkylation/activation and the active species' activity are indeed sensitive to olefin monomer concentration, as **cat.1**/MAO is highly active in ethylene polymerization at 10 atm but becomes essentially inactive when the ethylene pressure is reduced to 5 or 1 atm (entries 14 and 15, Table 1).

The 1-octene incorporation ratio was calculated based on high-temperature polymer ^{13}C NMR,[73,74] showing 0.83 and 0.32 mol% 1-octene incorporation in the copolymerization at 30 and 100 °C, respectively. This represents a rare example of limited Cr catalysts which are known to copolymerize α-olefins with ethylene.[47,75–78] End group analysis by ^{1}H NMR shows the presence of various olefinic end groups (vinyl, vinylidene, and 1,2-disubstituted olefinic) (Fig. S20–S23†).

The active species

This chromium catalyst exhibits well-controlled catalytic olefin polymerization behavior in terms of polymer M_w, $Đ$, and comonomer incorporation ratio, which is undoubtedly related to the type of active species and the reaction conditions. Due to the paramagnetic nature and rapidly interchanging oxidation state of the Cr metal center, understanding the exact structure of the Cr active species is often challenging.[36,41,79] UV-vis-NIR[26,32,41,53] and EPR[36,47] are two commonly used techniques, which we also used to probe the *in situ* generated active species mimicking the ethylene homo- and co-polymerization conditions at 30 °C and 100 °C in the absence/presence of the 1-octene monomer. As shown in Fig. S43,† **cat.1** in PhCl shows absorption at 29 000 cm^{-1}. Mixing **cat.1** and 10 equiv. of MAO in PhCl at 30 °C for 30 min results in a subtle shift to 29 300 cm^{-1}, and ethylene polymerization affords a low ratio of low M_w PE products under similar conditions. In contrast, increasing the mixing temperature to 100 °C or mixing **cat.1** with MAO (10 equiv.) in the presence of 1-octene (both at 30 and 100 °C), a sharp absorption peak at 29 300 cm^{-1} was observed with greater intensity, and predominantly low M_w polymers were obtained under similar conditions. This correlation may suggest that the new species as observed by UV-vis-NIR at 29 300 cm^{-1} is responsible for producing low M_w polymers in ethylene homo- and co-polymerization. The above samples were also studied by EPR but are unfortunately inconclusive due to the complicated catalyst system.

Conclusions

In conclusion, a novel tridentate phenoxy-phosphine (POP) Cr(II) complex based on the tridentate phenoxy-phosphine (POP) ligand was synthesized, characterized, and used for efficient ethylene, norbornene, and 1-octene homo- and copolymerization. Upon MAO activation, this catalyst shows tunable reactivities in terms of polyolefin M_w, dispersity ($Đ$), chain transfer capability, and chain termination pathways. Increasing MAO loading and reaction temperature changes the PE products from the predominant LMW fraction to the predominant HMW fraction. While β-H elimination is the predominant chain termination pathway in ethylene homo- and co-polymerization with NBE or 1-octene, chain transfer to $AlMe_3$ can become the exclusive pathway in NBE homopolymerization when β-H elimination is prohibitive; the resulting olefinic end groups from β-H elimination are derived from incorporating vinyl-terminated LMW polyolefin products or the 1-octene comonomer, which leads to vinylidene and 1,2-disubstituted olefinic end groups. All these processes are sensitive to MAO loading, reaction temperature, and monomer type and concentration, likely reflecting the sophisticated precatalyst alkylation/activation and active species generation processes and reaction condition-sensitive active species stability. UV-vis-NIR studies identified a new peak, the intensity of which correlates well with the active species responsible for low M_w polyolefin production under various conditions.

Experimental section

Materials and methods

Unless stated otherwise, all reactions with air- and moisture-sensitive materials were carried out under an inert gas atmosphere using standard glovebox and Schlenk techniques. Toluene and 1-octene were pre-dried over activated 4 Å molecular sieves and heated to reflux over sodium, and then stored over a Na/K alloy; NBE and THF were heated and refluxed over sodium, and then purified *via* distillation under a N_2 atmosphere. PhCl was refluxed over CaH_2 for 2 days, distilled under a N_2 atmosphere, and stored in a screw-capped Schlenk flask. Methylaluminoxane (MAO, 1.0 M in toluene) and modified methylaluminoxane (MMAO, 2.0 M in toluene) were purchased from Akzo Nobel. $AlEt_2Cl$, $AlEt_3$ (1.0 M in hexanes), Al^iBu_3 (1.0 M in hexanes), 1,1,2,2-tetrachloroethane-d_2, and other reagents were purchased from J&K Scientific.

Physical and analytical measurements

^{1}H NMR and ^{13}C NMR spectra were recorded on a Bruker 400 MHz NMR or Bruker 600 MHz NMR spectrometer. X-Ray crystallographic data were collected using a Bruker AXSD8 X-ray diffractometer. Elemental analysis was performed at the Analytical Laboratory of the Shanghai Institute of Organic Chemistry (CAS). UV-Vis-NIR spectra were recorded using a UV-3600 (Shimadzu). The spectra were measured in transmission mode using homemade cells equipped with an optical quartz window.

Synthesis of the ligand 2,6-bis(diphenylphosphino)-4-*tert*-butylphenol (L1) and Cr(II) complex cat.1

L1 was synthesized according to the previously published[43] procedure. ^{1}H NMR (400 MHz, $CDCl_3$): δ 7.35 (m, 20 H, Ar–*H*), 6.90–6.91 (d, 2 H, Ar–*H*), 6.37 (s, 1 H, O*H*), 0.97 (s, 9 H, –C*H*$_3$); ^{31}P NMR (161.9 MHz, $CDCl_3$): δ 20.84.

Cat.1: to a suspension of potassium hydride (KH, 0.072 g, 1.78 mmol, 1.2 equiv.) in dry THF (20 mL) was added a THF solution (25 mL) of **L1** (0.770 g, 1.48 mmol, 1.0 equiv.) at −30 °C. The resulting suspension was allowed to warm to room temperature while being stirred for 2 h, and after filtration over Celite, $CrCl_2$ (0.364 g, 2.96 mmol, 2.0 equiv.) was added to the solution, and the mixture was stirred overnight with the color turning to green. After filtration over Celite, all the volatiles were removed under reduced pressure to afford a green mixture, and the resulting mixture was redissolved in dry THF, and then crystallized from a mixed THF and *n*-hexane solution (1/3 v/v) to afford **cat.1** as a green solid, 0.462 g, 42.9% yield. Single crystals suitable for X-ray diffraction studies were grown from saturated THF solution in a freezer (−30 °C). Crystal data and detection parameters for **cat.1** are summarized in Tables S3 and S4,† and the CCDC deposition number for **cat.1** is 2205183. Elem. Anal. Calcd for $C_{34}H_{31}Cl_3Cr_2OP_2$ (**cat.1**–2THF): C 56.10%, H 4.29%; found: C 55.51%, H 4.73%.

Procedure for ethylene homopolymerization

Entry 5 in Table 1 is used as an example to introduce the typical polymerization procedure. Toluene (20 mL) and MAO (10 mmol, half of the total amount used) were added to a 350 mL stainless reactor in a glovebox, and the reactor was sealed, taken out of the glovebox, and attached to a high vacuum/high-pressure line. The solution was saturated with 2 atm of ethylene and kept in an oil bath at 50 °C for 20 min for equilibration. The amount of toluene was adjusted to ensure that the total volume of the solution is 50 mL. Inside the glovebox, the Cr complex was dissolved in PhCl (10 mL) in a glass vial, to which MAO (10 mmol, half of the total amount used) was added. After shaking for 2 min, the catalyst solution was loaded in a disposable syringe equipped with a long needle capped with a rubber septum, taken out of the glovebox, and injected into the reactor. The reactor was immediately pressurized with 10 atm of ethylene to start the polymerization. After 0.5 h, the ethylene pressure was released and the polymerization was carefully quenched with methanol, and then the mixture was poured into acidified ethanol (300 mL, 10% v/v HCl in ethanol). The precipitated polymer was collected by filtration, washed with ethanol, and then dried under vacuum at 60 °C overnight until constant weight. *CAUTION: methanol should be injected into the reactor very slowly to quench the large excess of MAO and fast stirring was necessary to avoid generating a large volume of alkane gas and exotherm in a short period of time*.

Procedure for NBE homopolymerization

Entry 1 in Table 2 is used as an example to introduce the typical procedure for NBE homopolymerization. Toluene (12 mL) and MAO (10 mmol, half of the total amount used) were added to a 150 mL reactor in a glovebox, and then the reactor was sealed, taken out of the glovebox, and attached to a high vacuum/high-pressure line. To the reactor was added NBE (40 mmol, 5.0 M in toluene) under N_2 protection, and the solution was kept in an oil bath at 50 °C for 20 min for equilibration. Inside the glovebox, the Cr complex was dissolved in PhCl (10 mL) in a glass vial, and then MAO (10 mmol, half of the total amount used) was added. After shaking for 2 min, the catalyst solution was loaded in a disposable syringe equipped with a long needle capped with a rubber septum, taken out of the glovebox, and injected into the reactor. Other than that, the procedure is the same as procedure A.

Procedure for ethylene copolymerization with NBE or 1-octene

Entry 7 in Table 2 is used as an example to introduce the typical polymerization procedure for ethylene and NBE copolymerization. Toluene (12 mL) and MAO (10 mmol, half of the total amount used) were added to a 350 mL stainless reactor in a glovebox, and the reactor was sealed, taken out of the glovebox, and attached to a high vacuum/high-pressure line. The stainless reactor was saturated with 2 atm of ethylene and kept in an oil bath at 30 °C for 20 min for equilibration. The amount of toluene was adjusted to ensure that the total volume of the solution is 50 mL. Inside the glovebox, NBE (40 mmol, 5.0 M in toluene) was loaded in a disposable syringe equipped with a long needle capped with a rubber septum. The Cr complex was dissolved in PhCl (10 mL) in a glass vial, to which MAO (10 mmol, half of the total amount used) was added. After shaking for 2 min, the catalyst solution was loaded in a disposable syringe equipped with a long needle capped with a rubber septum, and the NBE (40 mmol, 5.0 M in toluene) loaded syringe was taken out of the glovebox together, and NBE was injected into the reactor first followed by the catalyst solution. Other than that, the procedure is the same as the procedure for ethylene homopolymerization.

Entry 9 in Table 2 is used as an example to introduce the typical polymerization procedure for ethylene and 1-octene copolymerization. Toluene (10.6 mL), MAO (10 mmol, half of the total amount used), and 1-octene (60 mmol, 9.42 mL) were added to a 350 mL stainless reactor in a glovebox, and the reactor was sealed, taken out of the glovebox, and attached to a high vacuum/high-pressure line. The stainless reactor was saturated with 2 atm of ethylene and kept in an oil bath at 30 °C for 20 min for equilibration. The amount of toluene was adjusted to ensure that the total volume of the solution is 50 mL. Inside the glovebox, the Cr complex was dissolved in PhCl (10 mL) in a glass vial, to which MAO (10 mmol, half of the total amount used) was added. After shaking for 2 min, the catalyst solution was loaded in a disposable syringe equipped with a long needle capped with a rubber septum, taken out of the glovebox, and injected into the reactor. Other than that, the procedure is the same as the procedure for ethylene homopolymerization.

UV-vis-NIR measurement

Inside a glovebox, 5 μmol of **cat.1** was dissolved in PhCl (40 mL) in a homemade cell equipped with an optical quartz window to prepare a solution (0.125 mM). For the samples with **cat.1** + MAO, MAO (10 equiv. per cat.) was added to the catalyst solution, heated for 30 min at 30 °C or 100 °C, sealed

with a Teflon plug, and taken out of the glovebox for immediate measurement; for the samples with **cat.1** + MAO + 1-octene, MAO (10 equiv. per cat.) and 1-octene (1000 equiv. per cat.) were added to a homemade cell, heated for 30 min at 30 °C or 100 °C, and taken out of the glovebox for immediate measurement.

Polymer characterization

NMR spectra were recorded on Bruker 400 MHz NMR and Bruker 600 MHz NMR spectrometers. Chemical shifts for ^{1}H and ^{13}C spectra were referenced using internal solvent resonances. ^{1}H and ^{13}C NMR analyses of the polymer microstructure were conducted in 1,1,2,2-tetrachloroethane-d_2 at 110 °C or 120 °C (as specified in the ESI†) with a delay time (d_1) of 20 s (for ^{1}H) and 10 s (for ^{13}C). The incorporation ratios of 1-octene[74] and NBE[80,81] were calculated according to the literature and olefinic and methyl chain end groups were not considered in the calculations. Polymer M_n, M_w, and $Đ$ were determined by GPC (Agilent Technologies PL-GPC 220, polystyrene calibration, 1,2,4-trichlorobenzene as the eluent at a flow rate of 1.0 mL min^{-1}) at 150 °C *via* an RI detector except for samples from entries 7 and 8 in Table 2 (Polymer Char with an IR detector, polystyrene calibration, 1,2-dichlorobenzene as the eluent at a flow rate of 1.0 mL min^{-1}, 150 °C). The RI detector is not suitable for these poly(ethylene-*co*-norbornene) samples.[82] GPC deconvolution was conducted using the Origin 2021 curve fitting function assuming that single-site catalytic behavior affords the polymer with a Schulz–Flory distribution of molecular weight ($Đ$). The $Đ$ constraint was removed to yield a better fit.[54] The weight percentages of the low and high molecular weight fractions (LMW and HMW) were estimated from the deconvolution of the corresponding polymer GPC traces.

Conflicts of interest

L. Ji, Y. Y. Zhou, X-L. Sun, Y. S. Gao and Y. Tang are inventors of a provisional patent application for the chromium complex and catalytic processes described herein.

Acknowledgements

The authors are grateful for the financial support from the National Key R&D Program of China (No. 2021YFA1501700) and the start-up fund from Southern University of Science and Technology, Guangdong Provincial Key Laboratory of Catalysis (2020B121201002). The authors acknowledge Prof. Feng He and Dr Liang Han of the Department of Chemistry, Southern University of Science and Technology for their kind help in the UV-vis-NIR measurement and analysis.

References

1 C. Copéret, F. Allouche, K. W. Chan, M. P. Conley, M. F. Delley, A. Fedorov, I. B. Moroz, V. Mougel, M. Pucino, K. Searles, K. Yamamoto and P. A. Zhizhko, *Angew. Chem., Int. Ed.*, 2018, **57**, 6398–6440.
2 R. Cheng, Z. Liu, L. Zhong, X. He, P. Qiu, M. Terano, M. S. Eisen, S. L. Scott and B. Liu, in *Polyolefins: 50 years after Ziegler and Natta I: Polyethylene and Polypropylene*, ed. W. Kaminsky, Springer Berlin Heidelberg, Berlin, Heidelberg, 2013, pp. 135–202.
3 M. P. McDaniel, *Adv. Catal.*, 2010, **53**, 123–606.
4 E. Groppo, C. Lamberti, S. Bordiga, G. Spoto and A. Zecchina, *Chem. Rev.*, 2005, **105**, 115–184.
5 C. Bariashir, C. Huang, G. A. Solan and W.-H. Sun, *Coord. Chem. Rev.*, 2019, **385**, 208–229.
6 M. K. Smith, *Curr. Org. Chem.*, 2006, **10**, 955–963.
7 D. J. Jones, V. C. Gibson, S. M. Green, P. J. Maddox, A. J. White and D. J. Williams, *J. Am. Chem. Soc.*, 2005, **127**, 11037–11046.
8 J. Klosin, P. P. Fontaine and R. Figueroa, *Acc. Chem. Res.*, 2015, **48**, 2004–2016.
9 M. C. Baier, M. A. Zuideveld and S. Mecking, *Angew. Chem., Int. Ed.*, 2014, **53**, 9722–9744.
10 C. Redshaw and Y. Tang, *Chem. Soc. Rev.*, 2012, **41**, 4484–4510.
11 L. R. Sita, *Angew. Chem., Int. Ed.*, 2009, **48**, 2464–2472.
12 G. W. Coates, P. D. Hustad and S. Reinartz, *Angew. Chem., Int. Ed.*, 2002, **41**, 2236–2257.
13 G. W. Coates, *Chem. Rev.*, 2000, **100**, 1223–1252.
14 E. Y. X. Chen and T. J. Marks, *Chem. Rev.*, 2000, **100**, 1391–1434.
15 S. Mark, A. Kurek, R. Mülhaupt, R. Xu, G. Klatt, H. Köppel and M. Enders, *Angew. Chem., Int. Ed.*, 2010, **49**, 8751–8754.
16 Y. B. Huang and G. X. Jin, *Dalton Trans.*, 2009, 767–769.
17 T. Xu, Y. Mu, W. Gao, J. Ni, L. Ye and Y. Tao, *J. Am. Chem. Soc.*, 2007, **129**, 2236–2237.
18 S. Derlin and W. Kaminsky, *Macromolecules*, 2008, **41**, 6280–6288.
19 B. J. Thomas, S. K. Noh, G. K. Schulte, S. C. Sendlinger and K. H. Theopold, *J. Am. Chem. Soc.*, 1991, **113**, 893–902.
20 B. J. Thomas and K. H. Theopold, *J. Am. Chem. Soc.*, 1988, **110**, 5902–5903.
21 D. J. Jones, V. C. Gibson, S. M. Green and P. J. Maddox, *Chem. Commun.*, 2002, 1038–1039.
22 C. Huang, S. Du, G. A. Solan, Y. Sun and W. H. Sun, *Dalton Trans.*, 2017, **46**, 6948–6957.
23 Z. Hao, B. Xu, W. Gao, Y. Han, G. Zeng, J. Zhang, G. Li and Y. Mu, *Organometallics*, 2015, **34**, 2783–2790.
24 M. A. Esteruelas, A. M. López, L. Méndez, M. Oliván and E. Oñate, *Organometallics*, 2003, **22**, 395–406.
25 L. A. MacAdams, G. P. Buffone, C. D. Incarvito, A. L. Rheingold and K. H. Theopold, *J. Am. Chem. Soc.*, 2005, **127**, 1082–1083.
26 J. Tian, X. Zhang, S. Liu and Z. Li, *Polym. Chem.*, 2022, **13**, 1852–1860.
27 D. S. McGuinness, *Chem. Rev.*, 2011, **111**, 2321–2341.
28 S. Licciulli, I. Thapa, K. Albahily, I. Korobkov, S. Gambarotta, R. Duchateau, R. Chevalier and K. Schuhen, *Angew. Chem., Int. Ed.*, 2010, **49**, 9225–9228.

29 O. L. Sydora, *Organometallics*, 2019, **38**, 997–1010.
30 A. Bollmann, K. Blann, J. T. Dixon, F. M. Hess, E. Killian, H. Maumela, D. S. McGuinness, D. H. Morgan, A. Neveling, S. Otto, M. Overett, A. M. Z. Slawin, P. Wasserscheid and S. Kuhlmann, *J. Am. Chem. Soc.*, 2004, **126**, 14712–14713.
31 D. S. McGuinness, P. Wasserscheid, W. Keim, D. Morgan, J. T. Dixon, A. Bollmann, H. Maumela, F. Hess and U. Englert, *J. Am. Chem. Soc.*, 2003, **125**, 5272–5273.
32 D. Wang, S. Zhou, Y. Liu, X. Kang, S. Liu, Z. Li and P. Braunstein, *Macromolecules*, 2022, **55**, 2433–2443.
33 L.-P. He, H.-L. Mu, B.-X. Li and Y.-S. Li, *J. Polym. Sci., Part A: Polym. Chem.*, 2010, **48**, 311–319.
34 L.-P. He, J.-Y. Liu, L. Pan, J.-Q. Wu, B.-C. Xu and Y.-S. Li, *J. Polym. Sci., Part A: Polym. Chem.*, 2009, **47**, 713–721.
35 I. Vidyaratne, G. B. Nikiforov, S. I. Gorelsky, S. Gambarotta, R. Duchateau and I. Korobkov, *Angew. Chem., Int. Ed.*, 2009, **48**, 6552–6556.
36 A. Jabri, C. Temple, P. Crewdson, S. Gambarotta, I. Korobkov and R. Duchateau, *J. Am. Chem. Soc.*, 2006, **128**, 9238–9247.
37 C. Temple, A. Jabri, P. Crewdson, S. Gambarotta, I. Korobkov and R. Duchateau, *Angew. Chem., Int. Ed.*, 2006, **45**, 7050–7053.
38 G. Ricci, M. Battistella and L. Porri, *Macromolecules*, 2001, **34**, 5766–5769.
39 T. Simler, P. Braunstein and A. A. Danopoulos, *Organometallics*, 2016, **35**, 4044–4049.
40 P. Ai, A. A. Danopoulos and P. Braunstein, *Organometallics*, 2015, **34**, 4109–4116.
41 B. L. Small, M. J. Carney, D. M. Holman, C. E. O'Rourke and J. A. Halfen, *Macromolecules*, 2004, **37**, 4375–4386.
42 Z. Liu, W. Gao, X. Liu, X. Luo, D. Cui and Y. Mu, *Organometallics*, 2011, **30**, 752–759.
43 A. Beganskiene, N. I. Nikishkin, R. L. Luck and E. Urnezius, *Heteroat. Chem.*, 2006, **17**, 656–663.
44 A. Reinholdt, O. Staples and D. J. Mindiola, in *Comprehensive Coordination Chemistry III*, ed. E. C. Constable, G. Parkin and L. Que Jr, Elsevier, Oxford, 2021, pp. 478–507.
45 A. Jabri, P. Crewdson, S. Gambarotta, I. Korobkov and R. Duchateau, *Organometallics*, 2006, **25**, 715–718.
46 H. B. Hansen, H. Wadepohl and M. Enders, *Eur. J. Inorg. Chem.*, 2021, **2021**, 1278–1286.
47 T. Song, X. Tao, X. Tong, N. Liu, W. Gao, X. Mu and Y. Mu, *Dalton Trans.*, 2019, **48**, 4912–4920.
48 Q. Zheng, D. Zheng, B. Han, S. Liu and Z. Li, *Dalton Trans.*, 2018, **47**, 13459–13465.
49 P. Qiu, R. Cheng, B. Liu, B. Tumanskii, R. J. Batrice, M. Botoshansky and M. S. Eisen, *Organometallics*, 2011, **30**, 2144–2148.
50 S. Jie, R. Pattacini, G. Rogez, C. Loose, J. Kortus and P. Braunstein, *Dalton Trans.*, 2009, 97–105.
51 I. Vidyaratne, G. B. Nikiforov, S. I. Gorelsky, S. Gambarotta, R. Duchateau and I. Korobkov, *Angew. Chem. Int. Ed.*, 2009, **48**, 6552–6556.
52 S. V. Kulangara, D. Haveman, B. Vidjayacoumar, I. Korobkov, S. Gambarotta and R. Duchateau, *Organometallics*, 2015, **34**, 1203–1210.
53 G. Zanchin, A. Piovano, A. Amodio, F. De Stefano, R. Di Girolamo, E. Groppo and G. Leone, *Macromolecules*, 2021, **54**, 1243–1253.
54 R. D. Froese, P. D. Hustad, R. L. Kuhlman and T. T. Wenzel, *J. Am. Chem. Soc.*, 2007, **129**, 7831–7840.
55 C. Huang, A. Vignesh, C. Bariashir, Q. Mahmood, Y. Ma, Y. Sun and W.-H. Sun, *J. Polym. Sci., Part A: Polym. Chem.*, 2019, **57**, 1049–1058.
56 Y. Gao, M. D. Christianson, Y. Wang, M. P. Coons, J. Chen, J. Zhang, S. Marshall, T. L. Lohr, J. Klosin and T. J. Marks, *ACS Catal.*, 2022, **12**, 7589–7597.
57 T. Gunasekara, J. Kim, S. Xiong, A. Preston, D. K. Steelman, G. A. Medvedev, W. N. Delgass, J. M. Caruthers and M. M. Abu-Omar, *Macromolecules*, 2017, **50**, 9151–9161.
58 Y. Gao, J. Chen, Y. Wang, D. Pickens, A. Motta, Q. J. Wang, Y.-W. Chung, T. L. Lohr and T. J. Marks, *Nat. Catal.*, 2019, **2**, 236–242.
59 Q. Zhang, N. Wu, J. Xiang, G. A. Solan, H. Suo, Y. Ma, T. Liang and W.-H. Sun, *Dalton Trans.*, 2020, **49**, 9425–9437.
60 H. Terao, S. I. Ishii, J. Saito, S. Matsuura, M. Mitani, N. Nagai, H. Tanaka and T. Fujita, *Macromolecules*, 2006, **39**, 8584–8593.
61 E. Schiebel, M. Voccia, L. Falivene, L. Caporaso and S. Mecking, *ACS Catal.*, 2021, **11**, 5358–5368.
62 R. J. Sifri, O. Padilla-Vélez, G. W. Coates and B. P. Fors, *J. Am. Chem. Soc.*, 2020, **142**, 1443–1448.
63 C. Zou, S. Y. Dai and C. L. Chen, *Macromolecules*, 2018, **51**, 49–56.
64 M. Stürzel, S. Mihan and R. Mülhaupt, *Chem. Rev.*, 2016, **116**, 1398–1433.
65 D. A. Barnes, G. M. Benedikt, B. L. Goodall, S. S. Huang, H. A. Kalamarides, S. Lenhard, L. H. McIntosh, K. T. Selvy, R. A. Shick and L. F. Rhodes, *Macromolecules*, 2003, **36**, 2623–2632.
66 G. M. Benedikt, E. Elce, B. L. Goodall, H. A. Kalamarides, L. H. McIntosh, L. F. Rhodes, K. T. Selvy, C. Andes, K. Oyler and A. Sen, *Macromolecules*, 2002, **35**, 8978–8988.
67 H. Gao, S. Chen, B. Du, Z. Dai, X. Lu, K. Zhang, L. Pan, Y. Li and Y. Li, *Polym. Chem.*, 2022, **13**, 245–257.
68 L. Boggioni, D. Sidari, S. Losio, U. M. Stehling, F. Auriemma, A. Malafronte, R. Di Girolamo, C. De Rosa and I. Tritto, *Polymers*, 2019, **11**, 554.
69 L. Boggioni, D. Sidari, S. Losio, U. M. Stehling, F. Auriemma, R. Di Girolamo, C. De Rosa and I. Tritto, *Eur. Polym. J.*, 2018, **107**, 54–66.
70 N. Ni Bhriain, H. H. Brintzinger, D. Ruchatz and G. Fink, *Macromolecules*, 2005, **38**, 2056–2063.
71 A. Ravasio, L. Boggioni and I. Tritto, *Macromolecules*, 2011, **44**, 4180–4186.
72 H. Zhao, A. Ariafard and Z. Lin, *Inorg. Chim. Acta*, 2006, **359**, 3527–3534.

73 Y. Gao, M. D. Christianson, Y. Wang, J. Chen, S. Marshall, J. Klosin, T. L. Lohr and T. J. Marks, *J. Am. Chem. Soc.*, 2019, **141**, 7822–7830.
74 Y. Gao, A. R. Mouat, A. Motta, A. Macchioni, C. Zuccaccia, M. Delferro and T. J. Marks, *ACS Catal.*, 2015, **5**, 5272–5282.
75 M. Ronellenfitsch, T. Gehrmann, H. Wadepohl and M. Enders, *Macromolecules*, 2017, **50**, 35–43.
76 L. Pei, Y. Tang and H. Gao, *Polymers*, 2016, **8**, 69.
77 T. J. Woodman, Y. Sarazin, S. Garratt, G. Fink and M. Bochmann, *J. Mol. Catal. A: Chem.*, 2005, **235**, 88–97.
78 M. A. Esteruelas, A. M. López, L. Méndez, M. Oliván and E. Oñate, *New J. Chem.*, 2002, **26**, 1542–1544.
79 Y. Shaikh, J. Gurnham, K. Albahily, S. Gambarotta and I. Korobkov, *Organometallics*, 2012, **31**, 7427–7433.
80 M. Zhao and C. Chen, *ACS Catal.*, 2017, **7**, 7490–7494.
81 I. Tritto, C. Marestin, L. Boggioni, L. Zetta, A. Provasoli and D. R. Ferro, *Macromolecules*, 2000, **33**, 8931–8944.
82 A. L. McKnight and R. M. Waymouth, *Macromolecules*, 1999, **32**, 2816–2825.